

ULTRA-STABLE Hg⁺ TRAPPED ION FREQUENCY STANDARD*

J. D. Prestage, G. J. Dick, L. Maleki

California Institute of Technology, Jet Propulsion Laboratory
4800 Oak Grove Drive
Pasadena, California 91109

Abstract

We are developing a fieldable trapped ion frequency standard based on ¹⁹⁹Hg⁺ ions confined in a hybrid rf/dc linear ion trap. This trap permits storage of large numbers of ions with reduced susceptibility to the second-order Doppler effect caused by the rf confining fields. In preliminary measurements we have obtained a stability of $2-3 \cdot 10^{-15}$ for 10,000 second averaging times. These measurements were carried out with a 120 mHz wide atomic resonance line for the 40.5 GHz clock transition with a second order Doppler shift from the rf trapping field of $6 \cdot 10^{-13}$.

INTRODUCTION

Atomic frequency standards with high stability for averaging times τ longer than 1000 seconds are necessary for a variety of astrophysical measurements and long baseline spacecraft ranging experiments. The millisecond pulsar, PSR 1937+27, shows stability in its rotational period that exceeds that of all man-made clocks for averaging times longer than 6 months. Comparison of this pulsar period with an earth based clock of stability $1 \cdot 10^{-15}$ over averaging periods of one year is expected to show the effects of very low frequency gravitational waves[1,2]. Spacecraft ranging measurements across the solar system would be improved with earth based clocks whose stabilities exceeded $1 \cdot 10^{-15}$ for averaging times of 10^4 to 10^5 seconds. This clock performance would also improve gravity wave searches in spacecraft ranging data. Another use for long term stable clocks in NASA's Deep Space Network would be in maintaining syntonization with UTC.

We are developing a fieldable frequency standard based on ¹⁹⁹Hg⁺ ions confined in a linear ion trap which should show good long term frequency stability. Typically the largest source of frequency offset stems from the motion of the ions caused by the trapping fields via the second-order Doppler or relativistic time dilation effect. Though a large ion number is desirable for good signal to noise, the frequency offset which also grows with the number of ions forces us into a trade-off situation where fewer ions are trapped in order to reduce the (relatively) large offset and frequency instabilities which may result.

*This work represents the results of one phase of research carried out at the Jet Propulsion Laboratory, California Institute of Technology, under contract sponsored by the National Aeronautics and Space Administration.

In a conventional hyperbolic or Paul trap ions are trapped around the point node of the rf electric field at the center (Fig. 1). The strength of the electric field and the resulting micromotion of the trapped particles grows linearly with distance from this node point. As ions are added the size of ion cloud grows until the second order Doppler shift arising from the micromotion in the trapping field dominates the second order Doppler shift from the ion's thermal motion at room temperature. For typical operating conditions [3,13] a spherical cloud containing $2 \cdot 10^6$ mercury ions shows a 2nd order Doppler shift of $2 \cdot 10^{-12}$, a value some ten times larger than that for mercury ions undergoing room temperature thermal motion.

In order to increase the number of stored ions with no corresponding increase in second-order Doppler shift from ion micromotion we have designed and are currently testing a hybrid rf/dc linear ion trap. This trap confines ions along a line of nodes of the rf field (Fig.2). The trapping force transverse to the line of nodes is generated by the ponderomotive force as in conventional Paul traps while the axial trapping force is provided by dc electric fields [3-7].

We can compare the second-order Doppler shift, $\Delta f/f$ generated by the trapping fields for a cloud of ions in a linear trap and a conventional Paul trap [3,4] assuming that both traps are operated so that the ions have the same secular frequency ω . When the same number of ions N , are held in both traps the average distance from an ion to the node line of the trapping field is greatly reduced in the linear trap. Since the perpendicular distance from the line of nodes determines the magnitude of the rf trapping field the 2nd order Doppler shift of an ion's transition frequency due to motion in the trapping field is reduced from that of a conventional point node trap. If R_{sph} is the ion cloud radius in the Paul trap and L is the ion cloud length in the linear trap the Doppler shift in the two traps are related by[3]

$$\left(\frac{\Delta f}{f} \right)_{lin} = \frac{5}{3} \frac{R_{sph}}{L} \left(\frac{\Delta f}{f} \right)_{sph}. \quad (1)$$

As more ions are added to the linear trap this shift will increase. It will equal that of the spherical ion cloud in a hyperbolic trap when

$$N_{lin} = \frac{3}{5} \frac{L}{R_{sph}} N_{sph}. \quad (2)$$

Equations (2) and (3) are valid when the ion cloud radii, R_{lin} and R_{sph} , are much larger than the Debye length which is the characteristic plasma density fall off length at the ion cloud edge and is about 0.4 mm for typical Hg^+ ion plasmas used in frequency standard work [3,13].

In addition to its larger ion storage capacity the dependence of the second-order Doppler shift on trapping parameters in a linear trap is very different from that in a conventional Paul trap. For many ions in a Paul trap this shift is given by[3,10]

$$\left(\frac{\Delta f}{f} \right)_{sph} = -\frac{3}{10c^2} \left(\frac{N\omega q^2}{4\pi\epsilon_0 m} \right)^{2/3} \quad (3)$$

where ω is the secular frequency for a spherical ion cloud containing N ions each with charge to mass ratio q/m . c is the speed of light and ϵ_0 is the permittivity of free space. Ions in a linear trap show a 2nd order Doppler shift from the motion generated by the rf confining field given by[3]

$$\left(\frac{\Delta f}{f}\right)_{lin} = -\left(\frac{q^2}{8\pi\epsilon_0 mc^2}\right)\frac{N}{L} \quad (4)$$

where L is the length of the ion cloud.

In contrast to the spherical case as described Eq.(3), this expression contains no dependence on trapping field strength, as characterized by ω , and depends only on the linear ion density N/L. If for example, the rf confining voltage increases and consequently the micromotion at a given point in space increases, the ion cloud radius will decrease so that the second-order Doppler shift from ion micromotion remains constant. Similar statements can be made about variations in any parameter that effects the radial confinement strength [4].

The sensitivity of the finite length linear trap to variations in radial trapping strength (characterized by ω) is [4]

$$\frac{\delta\left(\frac{\Delta f}{f}\right)_{lin}}{\left(\frac{\Delta f}{f}\right)_{lin}} = -2\frac{R_t}{L}\frac{\delta\omega}{\omega}, \quad (5)$$

and to variations in endcap voltage is

$$\frac{\delta\left(\frac{\Delta f}{f}\right)_{lin}}{\left(\frac{\Delta f}{f}\right)_{lin}} = 2 \cdot \frac{R_t}{L} \frac{\delta V_e}{V_e} \quad (6)$$

where R_t is the trap radius. The Paul trap shows a corresponding sensitivity to trap field strength variations

$$\frac{\delta\left(\frac{\Delta f}{f}\right)_{sph}}{\left(\frac{\Delta f}{f}\right)_{sph}} = -\frac{2}{3}\frac{\delta\omega}{\omega}. \quad (7)$$

A comparison of Eqs. (5) and (7) shows the linear trap based frequency standard to be less sensitive to variations in trapping field strength than the Paul trap by a factor of $3R_t/L$. For the trap described in the next section this factor is about 1/3.

LINEAR TRAP DESCRIPTION

Our linear trap is shown in Fig. 3. The operation of the trap as a frequency standard is similar to previous work [9,10]. The ions are created inside the trap by an electron pulse along the trap axis which ionizes a neutral vapor of ^{199}Hg . A helium buffer gas (2×10^{-3} Pascal or 1.5×10^{-5} torr) collisionally cools the ions to near room temperature. Resonance radiation (194 nm) from a ^{202}Hg discharge lamp optically pumps the ions into the F=0 hyperfine level of the ground state. This UV light is focused onto the central 1/3 of the 75 mm long ion cloud. The thermal motion of the ions along the length of the trap will carry all the ions through the light field so that pumping is complete in about 1.5 seconds for typical lamp intensities.

To minimize stray light entering the fluorescence collection system this state selection light is collected in a Pyrex horn as shown in Fig. 3. The placement of the LaB₆ electron filament is also chosen to prevent light from the white hot filament from entering the collection system. Its placement and relatively cool operating temperature together with good filtering of the state selection/interrogation

UV light in the input optical system have allowed frequency standard operation without the use of a 194 nm optical bandpass filter in the collection arm. This triples data collection rates since such filters typically have about 30% transmission for 194 nm light.

Microwave radiation (40.5 GHz) propagates through the trap perpendicular to the trap axis thereby satisfying the Lamb-Dicke requirement that the spatial extent of the ion's motion along the direction of propagation of the microwave radiation be less than a wavelength. This radiation enters the trap region through the Pyrex horn (see Fig. 3) and propagates in the opposite direction to the UV state selection/interrogation light. This allows fluorescence collection in both directions perpendicular to the plane of the page in Fig.3. For the resonance and stability data shown below fluorescence was collected in only one of these two directions.

FREQUENCY STANDARD OPERATION

We have used Ramsey's technique of successive oscillatory fields to probe the approximately 40.5 GHz clock transition in $^{199}\text{Hg}^+$ ions confined to the linear trap described above. In these measurements the 40.5 GHz signal is derived from an active Hydrogen maser frequency source as shown in Fig. 4. A representative resonance line used in the $^{199}\text{Hg}^+$ clock transition is shown in Fig. 5. State selection and interrogation is accomplished during the 1.5 seconds following the lamp turn on. It is, of course, necessary to switch the light level to near zero to prevent light shifts and broadening of the clock transition. A background light level of about 300,000 per 1.5 second collection period has been subtracted to generate the resonance shown. The successive oscillatory field pulses consist of two 0.4 second microwave pulses separated by 3.5 second free precession period. The data shown is an average of ten 4 Hz wide scans with a 15 mHz frequency step size.

To determine the frequency stability of the overall system of ions, trap, microwave source, etc., we have locked the output frequency of the 40.5 GHz source to the frequency of the central peak of the resonance shown in Fig. 5 in a sequence of 2048 measurements. The time required for each measurement is about 6.9 seconds and the loop response time was 5 measurement cycles. By averaging the frequencies of 2^N adjacent measurements ($N=1,2,\dots,10$) we form the modified Allan variance. Two such stability measurements are shown in Fig.6. The frequency stability presented here has been extended to longer averaging times than previously reported [8] primarily through the addition of a triple layer of magnetic shields. Fig. 9 compares the present stability to other frequency standards including the active hydrogen masers used in JPL's Deep Space Network.

LOCAL OSCILLATOR REQUIREMENTS

One of the factors that can degrade the performance of passive atomic frequency standards is frequency fluctuations in the local oscillator (L.O.). The limitation due to this effect continues to the longest times, having the same $1/\sqrt{\tau}$ dependence on measuring time τ as the inherent performance of the standard itself. The cause of this effect is time variation of the sensitivity to L.O. fluctuations due to the interrogation process. This limitation was evaluated in a recent calculation for sequentially interrogated passive standards[10]. Since our trapped ion standard is of this type, the analysis should be directly applicable.

Additionally, effects inherent in operation of the feedback loop introduce a $1/\tau$ limitation to standard

performance which depends on the attack time t_a of the feedback loop.

Roughly speaking, the analysis shows that the local oscillator must have frequency stability at least as good as that of the standard itself, for a measuring time equal to the interrogation cycle time t_c . However, the effect may be reduced by use of a short dead time t_d and double-pulse interrogation. In that case, the instability induced by an L.O. with constant (flat) variance $\sigma_{LO}(\tau)$, is given approximately by [11,13]

$$\sigma_y(\tau) \approx \left(\frac{t_d}{t_c} \right) \sigma_{LO}(t_c) \sqrt{\frac{t_c}{\tau}}. \quad (8)$$

This instability will add in quadrature to that inherent in the standard itself. Thus, our trapped mercury ion frequency source with a performance of $\sigma_y(\tau) = 1.7 \cdot 10^{-13}/\sqrt{\tau}$, a cycle time of $t_c = 6.5$ seconds, and dead time of $t_d = 3.5$ seconds requires an L.O. with performance approximately given by $\sigma_{LO}(6.5) < 6.5/3.5 \cdot 1.7 \cdot 10^{-13}/\sqrt{6.5} \approx 1.24 \cdot 10^{-13}$. Longer cycle times and higher performance would place a more stringent burden on the L.O.

A crystal quartz L.O. with stability of $\sigma_y(\tau) \approx 1 \cdot 10^{-13}$ from 1 to 100 seconds is available commercially and could be combined with the trapped ion standard. Adding the instability given by Eq. 8 for this oscillator in quadrature with that for the trapped ion source itself predicts a combined stability of $\sigma_y = 2.2 \cdot 10^{-13}/\sqrt{\tau}$. With a loop attack time of $t_a = 35$ seconds, this performance would be achievable for times $\tau > (t_a \cdot 1/1.7)^2 = 425$ seconds.

While operation at the highest performance levels may place unattainable requirements on available crystal quartz local oscillators, application with a hydrogen maser, or other ultra-high stability source such as a high-Q cryogenic oscillator, could enable long term performance beyond 10^{-15} . However, in such an application, the hydrogen maser's frequency would not be steered to that of an independently operating trapped ion source. The maser's output signal would instead be used itself to interrogate the Hg^+ transition. Information thus gathered would be used to compensate for long term variation in the maser frequency.

SOURCES OF FREQUENCY INSTABILITY

We have measured the second order Doppler shift induced by the micromotion in the trapping fields in two ways—by measuring the ion cloud radius and by measuring the ion frequency as the ion number decays. Fig. 8 shows fluorescence from the ions as a masked PMT is swept across the focal plane of the imaging/collection system. Spatial variations in background light has been eliminated by subtracting light levels measured with ions in the trap from light levels with no ions present. Assuming a cylindrical ion cloud, a ray tracing analysis of the light falling on the PMT aperture shows that a 1.5 mm radius ion cloud gives a good fit to the experimental data (see Fig.8). With this ion cloud radius, trap operation at 50 kHz transverse secular frequency will yield a second order Doppler shift from the trapping field of $6 \cdot 10^{-13}$ [8].

An independent measurement of this frequency shift is shown in Fig. 9. This figure shows the time variation of the output frequency of the 40.5 GHz source when servoed to the $^{199}Hg^+$ clock transition. At the time shown by the arrow the electron pulse which fires at each measurement cycle is stopped. From that point on the number of ions in the trap is diminishing as the frequency is continuously tracked. Near the end of the run there are very few ions in the trap, though, enough to give a weak lock and a determination of the ion resonance frequency in the limit of low ion number where trapping field shifts approach ordinary thermal second order Doppler shifts [8]. The approximately 25 mHz

frequency shift in going from many ions to few ions is in good agreement with the $6 \cdot 10^{-13}$ value obtained from the ion cloud radius measurement described above. There was no active ion number stabilization used in any of the measurements described here.

The fractional sensitivity of the $^{199}\text{Hg}^+$ clock transition to magnetic field variations is nearly 1000 times less than that of hydrogen at the same operating field. For the present measurements the field was set at $5\mu\text{T}$ (50 mG). At this operating field the unshielded atomic sensitivity is $2.5 \cdot 10^{-13}$ per mG. To reach $5 \cdot 10^{-16}$ frequency stability the current in the Helmholtz field bias coils must be stable to $5 \cdot 10^{-5}$. To prevent ambient field disturbances from influencing the ion frequency the trap region is surrounded by a triple layer magnetic shield of shielding factor 10,000.

CONCLUSIONS

We have demonstrated the increased signal-to-noise and very good stability inherent in a linear ion trap based frequency standard. Clock operation with line $Q = 3.3 \cdot 10^{11}$ has achieved performance of $2-3 \cdot 10^{-15}/\sqrt{\tau}$ for $\tau = 10,000$ seconds. Line Q's as high as $1.3 \cdot 10^{12}$ have been measured [8], indicating consequent performance for this trap as high as $5 \cdot 10^{-14}/\sqrt{\tau}$ for $\tau > 150$ seconds. The requirement for local oscillator stability required to achieve this performance is quite stringent. However, controlling a hydrogen maser or cryogenic oscillator for long term stability improvements seems straightforward.

ACKNOWLEDGEMENT

We wish to thank Dave Seidel for taking the ion cloud radius optical data, Randy Berends for making ^{202}Hg lamps and Bob Tjoelker for carefully reading this manuscript.

REFERENCES

- [1] D. W. Allan, "A Study of Long Term Stability of Atomic Clocks", *Errata Proc. 19th Annual Precise Time and Time Interval (PTTI) Applications and Planning Meeting*, 375-380, 1987.
- [2] M. M. Davis, J. H. Taylor, J. M. Weisberg, and D. C. Backer, "High-precision timing observations of the millisecond pulsar PSR1937+21", *Nature* **315**, 547-550, 1985.
- [3] J. D. Prestage, G. J. Dick, L. Maleki, "New Ion Trap for Frequency Standard Applications", *J. Appl. Phys.* **66**, No. 3, 1013-1017, August 1989.
- [4] J. D. Prestage, G. R. Janik, G. J. Dick, and L. Maleki, "Linear Ion Trap for Second-Order Doppler Shift Reduction in Frequency Standard Applications", in *IEEE Trans. Ultrason. Ferroelec. Freq. Contr.*, **37**, 535-542, 1990.
- [5] G. R. Janik, J. D. Prestage, and L. Maleki, "Simple Analytic Potentials for Linear Ion Traps", *J. Appl. Phys.* **67**, No. 10, 6050-6055, May 1990.
- [6] H. G. Dehmelt, "Introduction to the Session on Trapped Ions," *Proc. 4th Symp. Frequency Standards and Metrology*, 286, 1989.

- [7] D. J. Wineland, J. C. Bergquist, J. J. Bollinger, W. M. Itano, D. J. Heinzen, S. L. Gilbert, C. H. Manney, and C. S. Weimer, "Progress at NIST Toward Absolute Frequency Standards Using Stored Ions", in *Proceedings of the 43rd Ann. Symposium on Frequency Control*, 143–150, 1989.
- [8] J. D. Prestage, G. J. Dick, and L. Maleki, "Linear Ion Trap Based Atomic Frequency Standard", to appear in *IEEE Trans. Instr. Meas.*, April, 1991.
- [9] J. D. Prestage, G. J. Dick, and L. Maleki, "The JPL Trapped Ion Frequency Standard Development, *Proc. 19th Annual Precise Time and Time Interval (PTTI) Applications and Planning Meeting*", 285–297, 1987.
- [10] L. S. Cutler, R. P. Giffard, P. J. Wheeler, and G. M. R. Winkler, "Initial Operational Experience with a Mercury Ion Storage Frequency Standard", in *Proc. 41st Ann. Symp. Freq. Control, IEEE Cat. No. 87CH2427-3*, 12–19, 1987.
- [11] G. J. Dick, "Calculation of Trapped Ion Local Oscillator Requirements," *Proc. 19th Annual Precise Time and Time Interval (PTTI) Applications and Planning Meeting*, 133–146 1988.
- [12] C. Audoin, V. Candelier, and N. Dimarcq, "A Limit to the Frequency Stability of Passive Frequency Standards," to appear in *IEEE Trans. Instr. Meas.*, April, 1991.
- [13] L. S. Cutler, R. P. Giffard, and M. D. McGuire, "Thermalization of ^{199}Hg Ion Macromotion by a Light Background Gas in an RF Quadrupole Trap", *Appl. Phys. B* **36**, 137–142, 1985.
- [14] M. Jardino, M. Desaintfuscien, and F. Plumelle, "Prospects for a Mercury Ion Frequency Standard", *Jour. De Physique*, **C8**, 327–338, 1981.

FIGURE CAPTIONS

Figure 1 A conventional hyperbolic RF ion trap. A node of the RF and DC fields is produced at the origin of the coordinate system shown.

Figure 2 The rf electrodes for a linear ion trap. Ions are trapped along the line of nodes of the rf field with reduced susceptibility to second-order Doppler frequency shift.

Figure 3 Linear Ion Trap Assembly View. The trap is housed in a 3.375" vacuum cube. State selection light from the ^{202}Hg discharge lamp enters from the right, is focused onto the central 1/3 of the trap and is collected in the horn. Fluorescence from the trapped ions is collected in a direction normal to the page.

Figure 4 Schematic of measurement system where the $^{199}\text{Hg}^+$ clock frequency is compared to an H-maser frequency.

Figure 5 $^{199}\text{Hg}^+$ clock transition as measured with successive oscillatory fields method. This line shape results from two 0.4 second microwave pulses separated by a 3.5 second free precession period. The central line is about 120 mHz wide.

Figure 6 Two measurements of the $^{199}\text{Hg}^+$ clock transition stability for the 120 mHz resonance line of Figure 5. Fractional frequency stability is $2 \cdot 10^{-13}/\sqrt{\tau}$ for $35 < \tau < 10,000$ sec.

Figure 7 Comparison of the currently demonstrated $^{199}\text{Hg}^+$ stability with other frequency standards used in JPL's Frequency Standards Laboratory.

Figure 8 The ion cloud diameter as determined by sweeping a masked photomultiplier across the focal plane of the UV light imaging/collection system. The data displayed is collected light vs. detector position.

Figure 9 A direct measure of 2nd order Doppler shift due to ion motion in the rf trapping fields. As the ion number (and hence ion cloud radius) diminishes the clock frequency increases. A net frequency shift of 25 mHz ($6 \cdot 10^{-13}$) is shown.

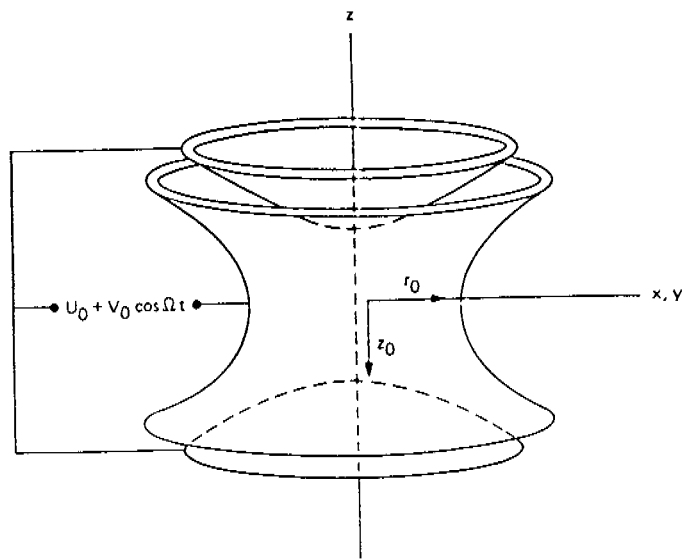


Figure 1 A conventional hyperbolic RF ion trap. A node of the RF and DC fields is produced at the origin of the coordinate system shown.

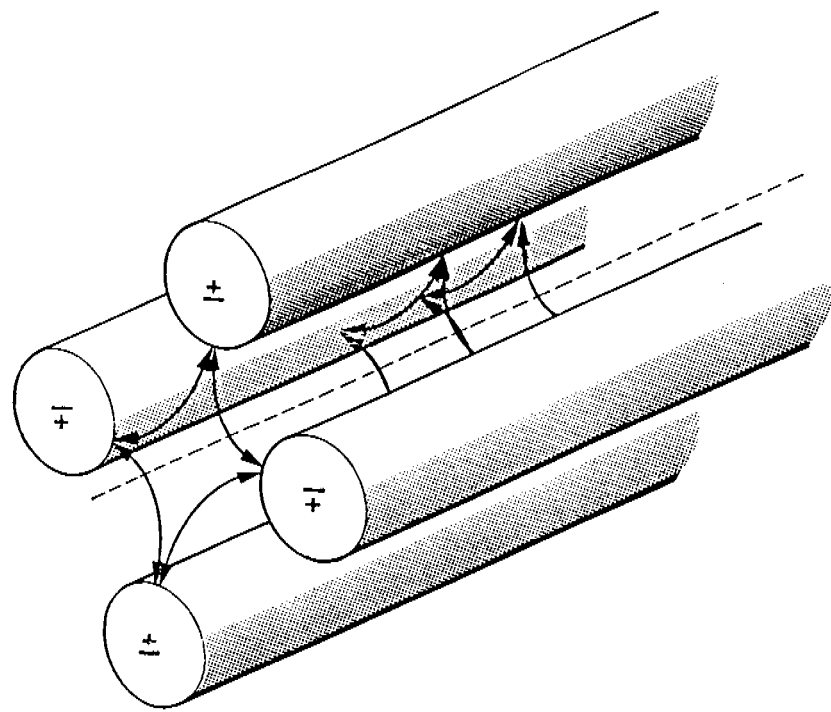


Figure 2 The rf electrodes for a linear ion trap. Ions are trapped along the line of nodes of the rf field with reduced susceptibility to second-order Doppler frequency shift.

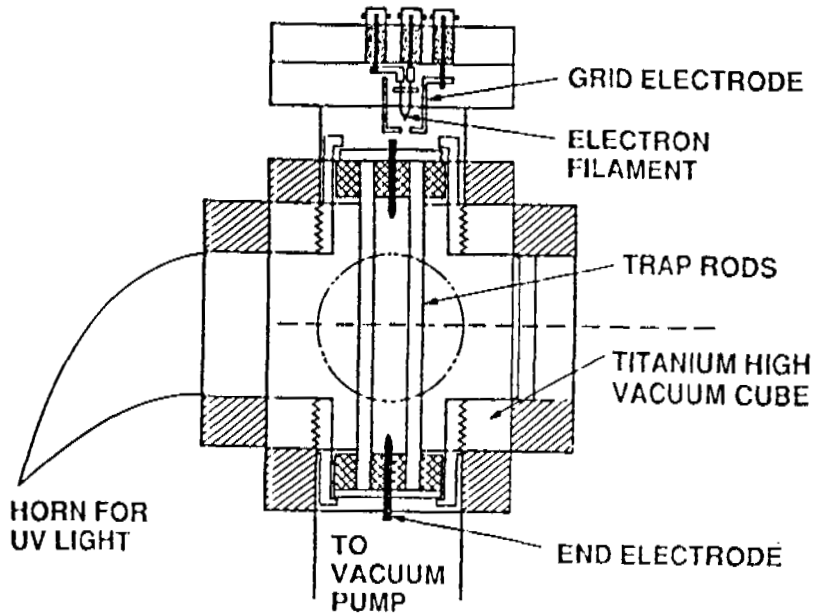


Figure 3 Linear Ion Trap Assembly View. The trap is housed in a 3.375" vacuum cube. State selection light from the ^{202}Hg discharge lamp enters from the right, is focused onto the central 1/3 of the trap and is collected in the horn. Fluorescence from the trapped ions is collected in a direction normal to the page.

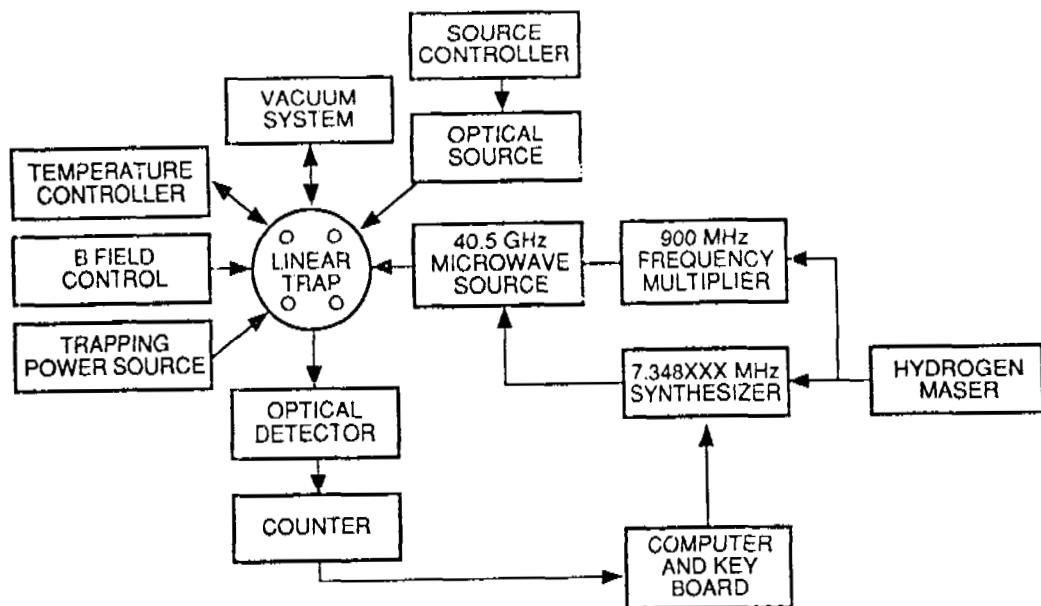


Figure 4 Schematic of measurement system where the $^{199}\text{Hg}^+$ clock frequency is compared to an H-maser frequency.

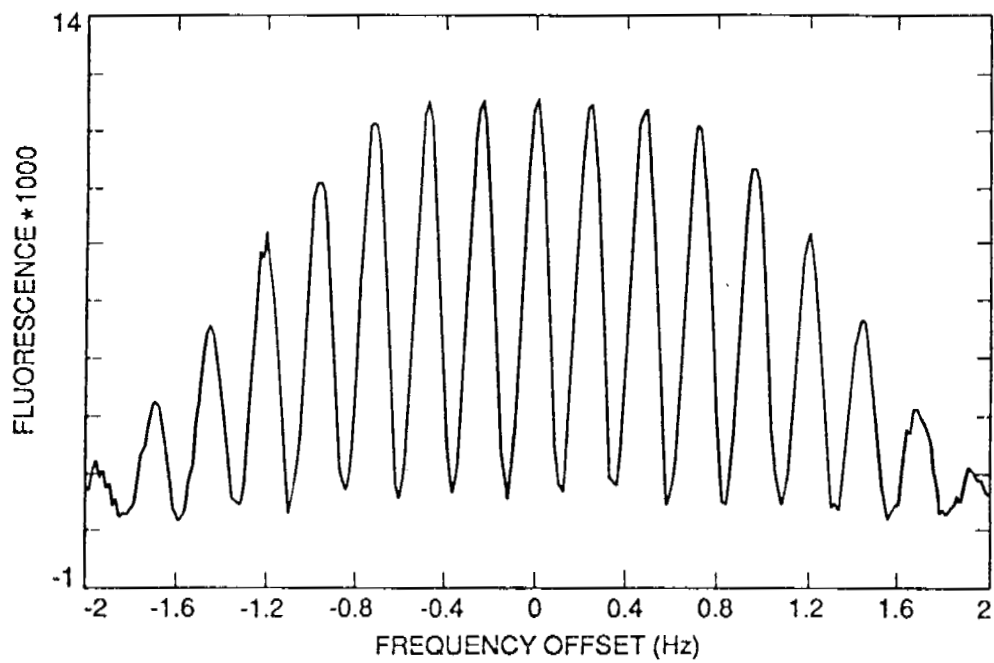
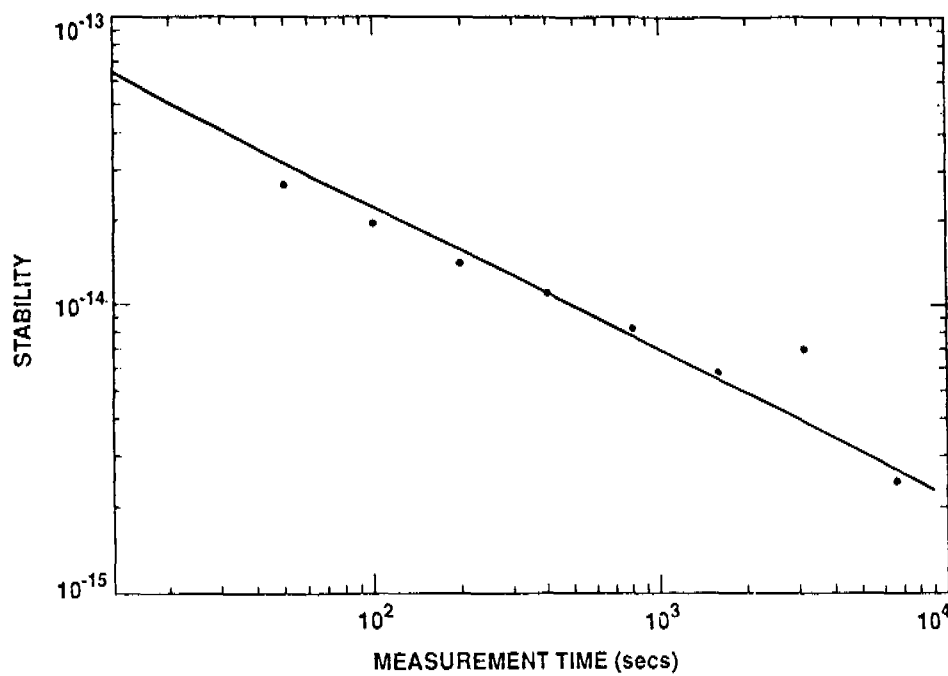


Figure 5 $^{199}\text{Hg}^+$ clock transition as measured with successive oscillatory fields method. This line shape results from two 0.4 second microwave pulses separated by a 3.5 second free precession period. The central line is about 120 mHz wide.

11/28/90 PM FLEXCO



11/29/90 AM FLEXCO

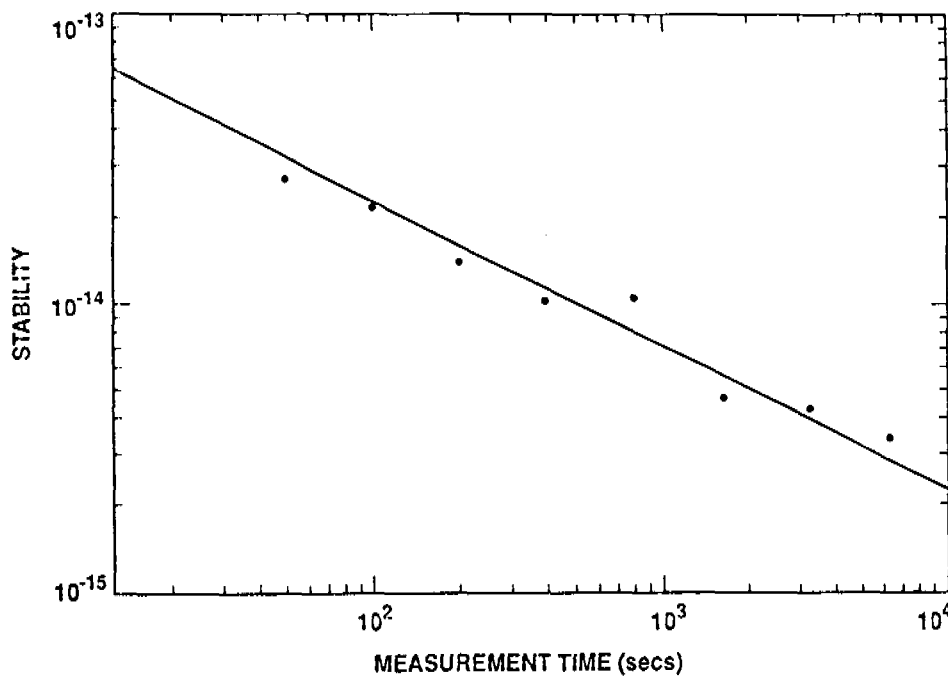


Figure 6 Two measurements of the $^{199}\text{Hg}^+$ clock transition stability for the 120 mHz resonance line of Figure 5. Fractional frequency stability is $2 \cdot 10^{-13}/\sqrt{\tau}$ for $35 < \tau < 10,000$ sec.

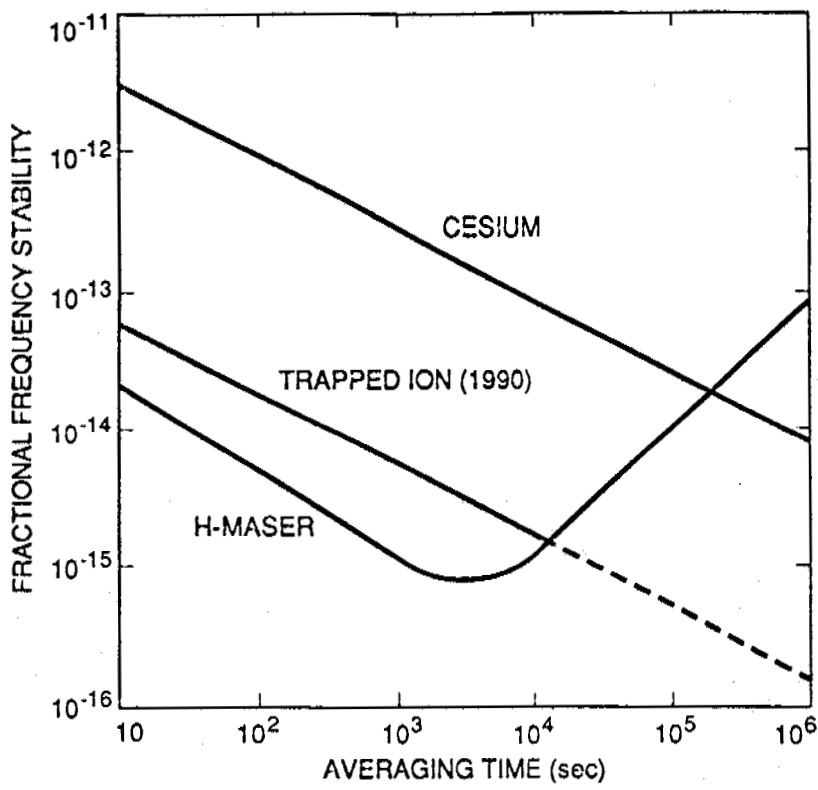


Figure 7 Comparison of the currently demonstrated $^{199}\text{Hg}^+$ stability with other frequency standards used in JPL's Frequency Standards Laboratory.

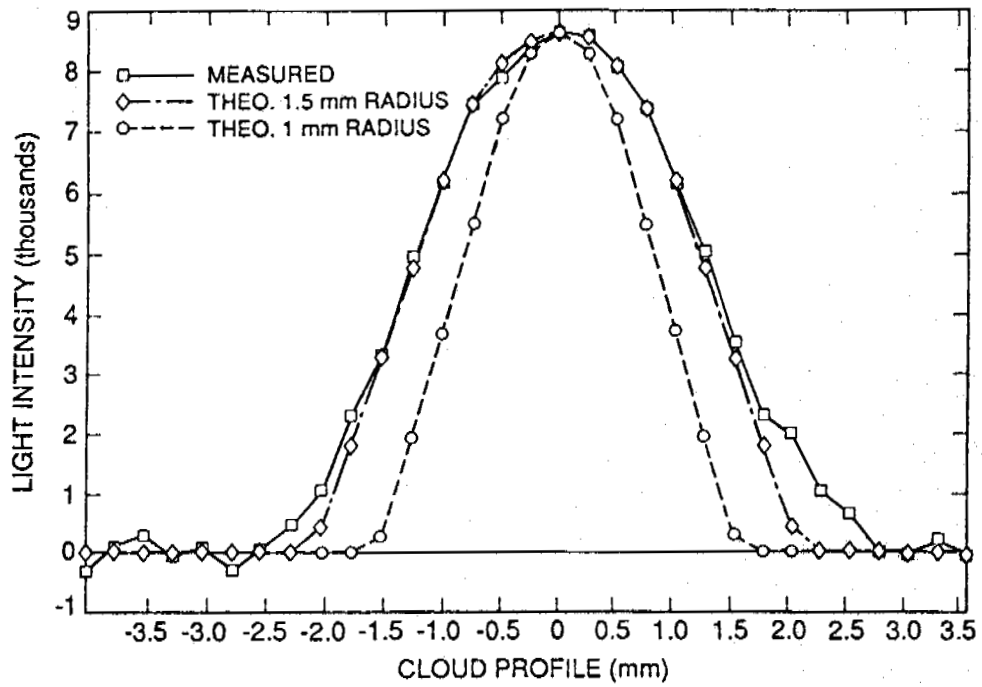


Figure 8 The ion cloud diameter as determined by sweeping a masked photomultiplier across the focal plane of the UV light imaging/collection system. The data displayed is collected light vs. detector position.

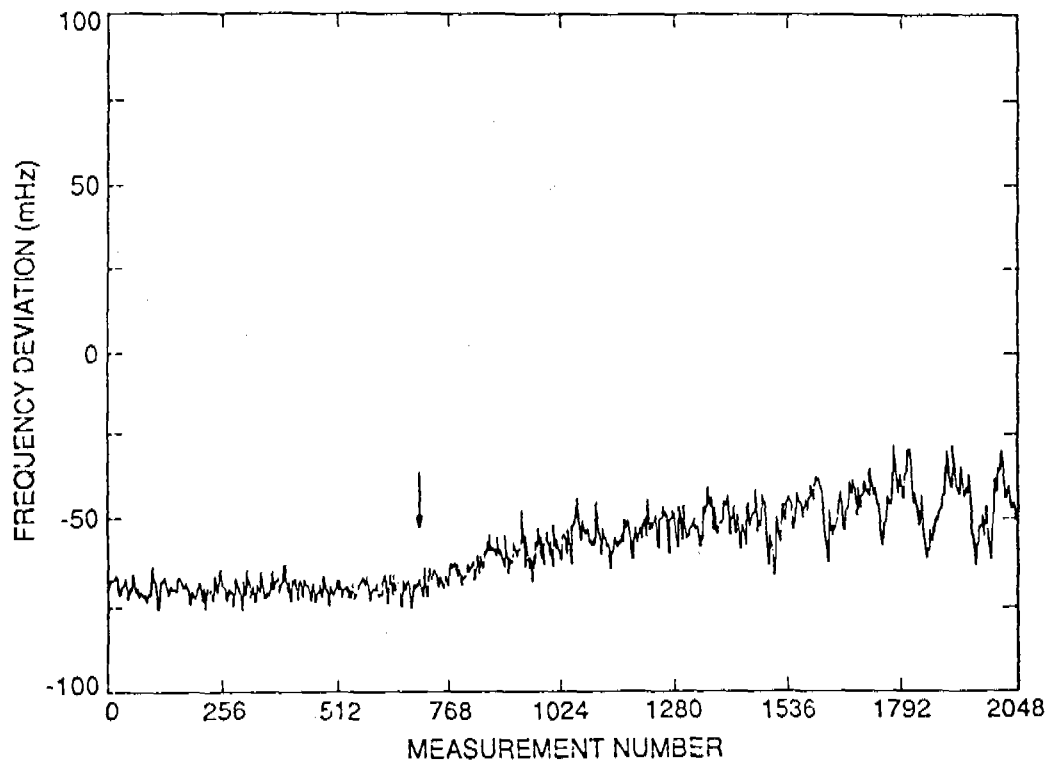


Figure 9 A direct measure of 2nd order Doppler shift due to ion motion in the rf trapping fields. As the ion number (and hence ion cloud radius) diminishes the clock frequency increases. A net frequency shift of 25 mHz ($6 \cdot 10^{-13}$) is shown.

QUESTIONS AND ANSWERS

Dr. Thomann, Neuchatel Observatory: How good a candidate would that be for a primary standard?

Dr. Prestage: As we run it the second order doppler shift is probably the limiting effect. Accuracy of 1×10^{-13} would be reasonable.

Dr. Thomann: By sacrificing some signal to noise you could improve the second order doppler effect significantly?

Dr. Prestage: Yes, we could.